Available online at www.sciencedirect.com
SCIENCE DIRECT®
Colloids and Surfaces B: Biointerfaces 31 (2003) 95–105
COLLOIDS AND SURFACES B
www.elsevier.com/locate/colsurfb

Foams and surface rheological properties of β-casein, gliadin and glycinin

Martin A. Bos [a,b,*], Bertus Dunnewind [a,b], Ton van Vliet [a]

[a] *Wageningen Centre for Food Sciences, Department of Food Science, C/o Wageningen University, Food Physics Group, P.O. Box 8129, EV Wageningen 6700, The Netherlands*
[b] *TNO Nutrition and Food Research Institute, P.O. Box 360, AJ Zeist 3700, The Netherlands*

Received 20 August 2002; received in revised form 6 November 2002; accepted 12 November 2002

Abstract

Interfacial rheological properties and their suitability for foam production and stability of two vegetable proteins were studied and compared to β-casein. Proteins used ranged from flexible to rigid/globular in the order of β-casein, gliadin and soy glycinin. Experiments were performed at pH 6.7. Network forming properties were characterised by the surface dilational modulus (determined with the ring trough) and the critical falling film length (L_{still}) at which a stagnant protein film will break. Gliadin had the highest dilational modulus, followed by glycinin and β-casein, whereas glycinin formed the strongest film against fracture in the overflowing cylinder. The rate of decrease in the surface tension was studied at the air–water (Wilhelmy plate method) and the oil–water interface (bursting membrane) and the dynamic surface tension during compression and expansion in the caterpillar. Gliadin had the lowest equilibrium interfacial tensions and β-casein the lowest dynamic surface tension during expansion. Hardly any foam could be formed at a concentration of 0.1 g/l by shaking. At a concentration of 1.4 g/l most foam was formed by β-casein, followed by gliadin and glycinin. It seems that in the first place the rate of adsorption is important for foam formation. For the vegetable proteins, adsorption was slow. This resulted in lower foamability, especially for glycinin.

Keywords: Foam formation; Foam stability; Surface rheology; Gliadin; Glycinin; β-Casein

1. Introduction

In the food industry, vegetable proteins play an important role in the formation and stabilisation of various foods, in which they are used as an interesting alternative for proteins from animal origin. Typical functions of these proteins are gel formation, emulsification, foaming, thickening, water absorption and water holding [1,2].

During the formation and stabilisation of emulsions and foams, interfaces behave dynamically; they are expanded and/or compressed. Therefore, it is important to study the behaviour of adsorbed proteins under dynamic conditions.

* Corresponding author. Tel.: +30-69-44174; fax: +30-69-57224.
E-mail address: m.bos@voeding.tno.nl (M.A. Bos).

0927-7765/03/$ - see front matter © 2003 Elsevier B.V. All rights reserved.
doi:10.1016/S0927-7765(03)00046-8

Extensive interfacial rheological studies have been performed for several well-known proteins, like cow milk proteins (especially β-casein and β-lactoglobulin), bovine serum albumin, ovalbumin and lysozyme [3–7]. However, vegetable proteins like those of wheat and soy, often used in applications where bulk rheological properties are most important, have only preliminary been studied. In these studies, the focus was on the interactions with (phospho)lipids in case of wheat gliadins and/or glutelins [3,8–11] and on the effects of modification of soy glycinin [12–14]. Martin and co-workers [15] showed for soy glycinin the importance of the conformation of the glycinin molecules for the surface rheological properties.

Since vegetable proteins may form an interesting alternative for proteins from animal origin for use in foams and emulsions, in this study the surface rheological properties of gliadin and glycinin will be compared with those of β-casein. Surface dilational parameters at the air–water interface were determined both at small oscillatory deformations and large steady-state deformations. As a first step to practical applications, foaming behaviour was determined and related to the surface properties.

2. Materials and methods

2.1. Protein solutions

β-Casein (Sigma) was dissolved in 30 mg/ml 10-mM phosphate buffer (pH 7.0) and applied at 4 °C to a fast-desalting column (PD-10, Pharmacia) according to manufacturer's instructions. The pooled protein fraction was subsequently dialysed against demineralised water, freeze-dried and stored at −20 °C until further use.

Glycinin was isolated from soybeans (Williams 82; 1994 harvest) principally according to the fractionation described by Tanh and Shibasaki [17] with some adaptations as described by Lakemond et al. [18]. Protein (>95% purity) was stored in a concentration of approximately 35 mg/ml in 10 mM phosphate buffer (pH 6.8) containing 20% glycerol at −40 °C.

A gliadin fraction was obtained by extraction of a rinsed wheat gluten fraction with an acetic acid aqueous solution (pH 4.0) for 12 h at 4 °C. After homogenisation of the material and subsequent centrifugation (60 min at $27\,500 \times g$ and 10–15 °C), 5 M NaCl was added to a final salt concentration of 75 mM. After incubation for 12 h at 4 °C, the precipitated material was removed by centrifugation (60 min at $27\,500 \times g$ at 10–15 °C). Gel electrophoretic analysis of the protein composition of the supernatant demonstrated that the gliadin fraction was obtained. 20% glycerol was added to the supernatant and the material was stored at −40 °C until further use.

Prior to use, glycinin and gliadin batches were defrosted at room temperature and dialysed to remove glycerol. Dialysis tubings with a molecular weight cut-off of 12 000–14 000 Da (Visking) were first boiled for at least 10 min in demineralised water in the presence of 5 mM EDTA and subsequently rinsed extensively with demineralised water. Prior to an experiment, gliadin or glycinin was defrosted and dialysed five times against a 100 times excess 20 mM phosphate buffer (pH 7.0) with at least 4 h between the dialysis buffer changes. While the first dialysis step was performed at 20 °C, others were carried out at 4 °C. Natural abundance ^{13}C NMR analysis of the dialysed material did not show any trace of glycerol in the samples (results not shown). The detection of glycerol present in the sample was based on the integration of NMR bands at 71–72 ppm assigned to glycerol and by comparison of the integral with that of a sample with a known amount of glycerol (10 mol per mol protein) added. The estimated detection limit was approximately 1 molecule of glycerol per protein.

2.2. Buffer solutions

Proteins were dissolved in phosphate buffer made with 1.18 g Na_2HPO_4 and 1.51 g NaH_2PO_4 per liter, using HCl to set pH to 6.7. The ionic strength of this buffer, calculated on the basis of dissociation constants, assuming complete dissociation of Na^+, was 30 mM. The conductivity was 2.01 mS/cm, measured on a microprocessor conductivity meter LF 537 of WTW, Weilheim,

Germany. All chemicals used were of analytical grade and were obtained from Merck (Germany).

All glasses were cleaned and extensively rinsed with tap water prior to use. Care was taken not to use anything containing synthetic material (except Teflon), as plasticizers appear to affect surface tension.

2.3. Sunflower oil

Sunflower oil was obtained from Smilde Food (The Netherlands) and was purified prior to usage. To remove surface-active components from the sunflower oil, 50 g silica gel (silica gel 60, particle size 0.063–0.200 mm, Merck, Germany) was dried at 110 °C for at least 1 h and added to 0.5 l sunflower oil in a beaker. The mixture was stirred under vacuum in a dessicator heated to 50 °C at 500 rpm for 1–2 h. Silica was removed by filtering under vacuum through a filter paper disc on a Büchner funnel (black ribbon filter paper discs from Schleicher & Schühl, Germany). Oil was poured in Erlenmeyer flasks and purged with N_2. The headspace was filled with N_2 and the closed flasks were stored at −40 °C until use. This purification resulted in an increase of the interfacial tension of the oil–water interface from 19 to 29 mN/m and this value did not change with time anymore.

2.4. Surface tension measurements

In all surface rheological experiments, the interfacial tension was measured by Wilhelmy plate technique, making use of a roughened optical glass plate of about 2 cm wide.

2.5. Ring trough measurements

Surface dilational moduli were measured by Ring Trough method as described by Kokelaar et al. [19]. The absolute surface dilational modulus $|E|$ ($|E| \equiv |\mathrm{d}\gamma/\mathrm{d}\ln A|$), which is a measure of the stiffness of the interfacial layer, was determined by applying a sinusoidal deformation of the surface area A and monitoring the resulting change in surface tension γ. After the protein solution was put into the trough, the surface was cleaned by suction and the dilational modulus $|E|$ and $\tan\theta$, the ratio between the viscous behaviour and elastic behaviour of the surface, was monitored for several hours. For an ideally elastic behaviour of an interfacial layer, $\tan\theta$ is zero. Measurements were performed at frequencies ranging from 5 to 200 MHz and the amplitude of the ring movement was 1 mm which implied a deformation of 3.6% of the total surface area. All measurements were performed in the linear region at 24 °C.

2.6. Overflowing cylinder experiments

The overflowing cylinder technique used in this study has been described by Bergink-Martens et al. [20] and Boerboom [21]. The overflowing cylinder consists of an inner cylinder through which the liquid is pumped at a constant flow rate. Liquid flows over the upper rim of the inner cylinder along the inner cylinder wall into the circular container formed by the inner and outer cylinder. From this vessel, the liquid is pumped back to the inner cylinder. The height difference between the level of the liquid in the outer cylinder and the rim is called the falling film length L [21]. At the top of the inner cylinder, the surface expands radially at a constant relative expansion rate $\mathrm{d}\ln A/\mathrm{d}t$. For water, $\mathrm{d}\ln A/\mathrm{d}t$ is independent of the falling film length while for surfactant solutions it is not. By increasing the length L of the falling film, $\mathrm{d}\ln A/\mathrm{d}t$ of an aqueous surfactant solution increases beyond the value for pure water, whereas below a certain value of L the expansion rate is lower than that of pure water. By decreasing L below a threshold value, the surface expansion stops completely. The critical falling film length at which this first occurs is called L_{still} ($\mathrm{d}\ln A/\mathrm{d}t \sim 0$). L_{still} depends strongly on the nature of the surfactant used [22] and characterises the ability of a surfactant to build up a network preventing the surface from flowing. Whether the surface expands or not and whether or not a network is formed depends not only on L, but also on the flow rate Q and on the age of the surface (time). A stagnant protein film is formed at a certain combination of L and Q; increasing L or Q will rupture the film. In this study, the flow rate Q was fixed. So measuring $\mathrm{d}\ln A/\mathrm{d}t$ going from high to low L can be

interpreted as stagnant film formation whereas going from low to high L is related to fracture of the protein layer.

The used flow rate was 31.4 cm^3/s and L varied from 0.5 to 3 cm. Temperature was kept constant at 22 °C.

2.7. Continuous expansion/compression measurements

The dynamic surface tension in steady-state expansion or compression was determined using a Langmuir trough with an endless belt with moving barriers ('caterpillar-through') [23]. Trough's dimensions were length × width × depth = 400 mm × 190 mm × 30 mm. Six Teflon barriers were mounted on the endless belt. By altering the direction of the moving caterpillar belt, the surface between the moving barriers and a fixed barrier could be either continuously expanded or compressed. Measurements were performed first in expansion going from highest to lowest expansion rate and then in compression from lowest to highest compression rate. The surface tension was measured at about 3 cm from the fixed barrier and taken at the end of the movement of a barrier, and so just before the next barrier took over. The relative deformation rate of the surface was calculated from the speed of the moving barriers at that moment and the accompanying length of the surface being 21 and 13 cm in expansion and compression, respectively. The surface dilational viscosity was calculated from the difference between the measured surface tension and the surface tension measured in the ring trough. Measurements were performed at 25 °C.

2.8. Bursting membrane measurements

Adsorption kinetics of proteins at an oil–water interface was determined according to the bursting membrane method of Stang et al. [24]. Membranes used for the bursting membrane were made from balloons and were kept in acetone for at least 1 day. 16.6 ml of phosphate buffer was poured on the membrane (10 mm height) and 45 ml purified sunflower oil was carefully poured on the buffer (25 mm height). The Wilhelmy plate was calibrated when hanging just above the oil–water interface as to avoid influences of the upward force exerted by the oil on the plate. A sharpened stiff wire pricked the membrane and the decrease in interfacial tension was followed for 2 h.

2.9. Foam test

Foams were prepared by firmly shaking 20 ml protein solution in a 130 ml tube during 10 s (about 40 up-down movements). The upper and lower levels of the foam were read and followed in time resulting in foam volume and amount of liquid in the foam. The drainage rate was calculated as the slope of ln(liquid in foam) against ln(time).

3. Results and discussion

3.1. Surface tension measurements

The adsorption rate of the three proteins at the air–water interface (concentration 0.1 g/l) was followed by measuring the decrease in surface tension γ (mN/m) with time (Fig. 1). Since there is already protein adsorbed at the interface before a decrease in surface tension can be monitored, the determined rate of adsorption is not the adsorption rate by which the first protein molecules adsorb at the interface. The decrease in surface tension on short adsorption times of the proteins increases in the line glycinin < gliadin < β-casein. Protein molecular size, structure and affinity to the interface influence the adsorption rate. Disordered, small and flexible proteins reduce the surface tension earlier and faster than ordered, rigid and larger proteins. Since the hydrophobicities vary not much between the proteins used, they cannot be responsible for differences observed. Therefore, the adsorption rate is mainly determined by molecular size and structure. The molecular weights of β-casein, gliadin and glycinin are 24, 58 and 350 kDa, respectively. The order in adsorption rate coincides with the order in protein molecular size. The structure of the protein also plays a role in the adsorption behaviour [25]. β-

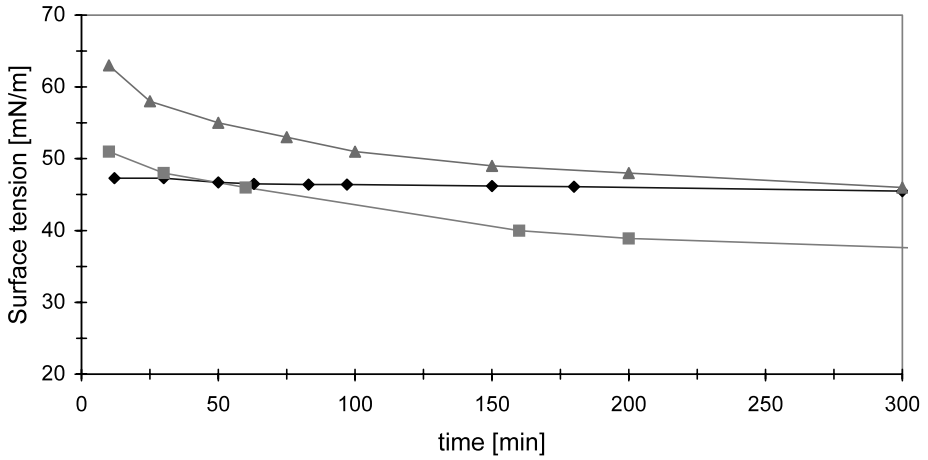

Fig. 1. Surface tension as a function of time at the air–water interface for β-casein (◆), gliadin (■) and glycinin (▲). Protein concentration was 0.1 g/l, pH 6.7.

Casein is a flexible, random-coil protein while gliadin and especially glycinin are compact globular proteins that likely unfold slower at an interface. This is also reflected in the change of the surface tension at longer time scales on top of the molecular size.

3.2. Ring trough

The surface dilational modulus E measured at the air–water interface increased in time (Fig. 2) for all three proteins. There is a fast increase up to 55 and 40 mN/m for gliadin and glycinin, respectively, after which the moduli increase at a lower rate. For β-casein, the increase in E is slowly over the time scale of the measurement. The maximum modulus reached by the proteins was in the order gliadin > glycinin > β-casein. The fast initial increase in E can be explained by an increase in the adsorbed amount, which is reflected in a decrease in surface tension (Fig. 1). The modulus of all three proteins still increased after ageing times that the surface tension did not change significantly anymore during the experiment. Probably, increased intermolecular interactions (due to conformational changes), beside some additional adsorption, are responsible for this increase at longer ageing times. Since gliadin is a mixture of proteins, the slow increase in the modulus could also be a result of displacement of one protein by another protein in the surface. In the case of glycinin, which is build up from six subunits, each of them consisting of one basic and one acidic polypeptide [18], the slowly increasing modulus above 40 mN/m might be due to the breakage of hydrophobic bonds. These hydrophobic bonds are involved in the stabilisation of the quaternary structure, and might be exposed to the surface [26]. The data for E and $\tan\theta$ presented are in good agreement with those mentioned in literature [27–30].

The dependence of E and $\tan\theta$ on the frequency is shown for the three proteins in Fig. 3. At the lowest frequency, the moduli for gliadin and glycinin were similar, but differences increased with increasing frequency. Glycinin formed a stiffer (higher E) and more elastic (lower $\tan\theta$) surface than β-casein. $\tan\theta$ decreased with increasing frequency for β-casein and especially for gliadin, but not for glycinin. The increase in E with increasing frequency was in the order glycinin < β-casein < gliadin (Fig. 3a). The strong dependence of E and $\tan\theta$ of gliadin on frequency could be a result of stronger diffusional relaxation, possibly due to the fact that gliadin is a mixture of proteins including puro-indolins [9].

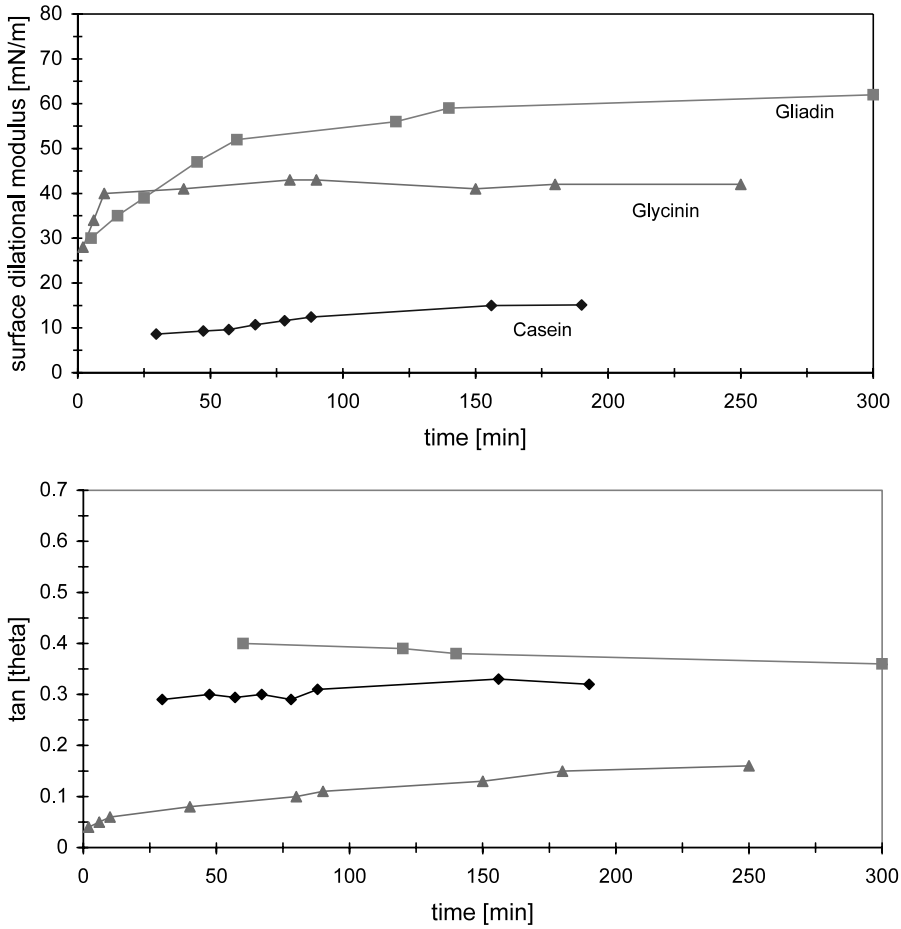

Fig. 2. Surface dilational modulus E and tan θ as a function of time t at the air–water interface at 0.1 Hz frequency and a strain of 3% measured in the ring trough for β-casein (◆), gliadin (■) and glycinin (▲). Protein concentration was 0.1 g/l, pH 6.7.

3.3. Overflowing cylinder

The maximum $\mathrm{d}\ln A/\mathrm{d}t$ at high L was slightly different for the different proteins (Fig. 4), being similar to $\mathrm{d}\ln A/\mathrm{d}t$ of tap water at the same flow rate ($\sim 1.7\ \mathrm{s}^{-1}$). Only β-casein reached slightly higher values. When the falling height L was decreased, the relative deformation rate $\mathrm{d}\ln A/\mathrm{d}t$ of the surface started to decrease at a similar value of L for all proteins. A large difference, however, was observed in the rate at which $\mathrm{d}\ln A/\mathrm{d}t$ decreased with decreasing L and in L at which $\mathrm{d}\ln A/\mathrm{d}t$ became zero. The rate was lower for β-casein and gliadin than for glycinin. The latter showed a very fast decrease of $\mathrm{d}\ln A/\mathrm{d}t$ to zero. Evidently proteins are able to slow down the motion of the surface drastically, but to a different extent. Below L_{still}, the radial surface expansion was completely counteracted likely due to the formation of an interfacial protein network. Visual observation showed that a network builds up from the cylindrical trough between the inner and outer cylinder where the surface was compressed. L_{still} can be considered as a measure for interfacial network formation under rough circumstances. At a flow rate of 31.4 cm^3/s and a protein concentration of 0.1 g/l, L_{still} increased in the order gliadin ≈ β-casein < glycinin with L_{still} being 1.7, 1.8 and 2.4 cm, respectively. Increasing L (from L_{still} on) leads to protein film rupture; L_{still} can

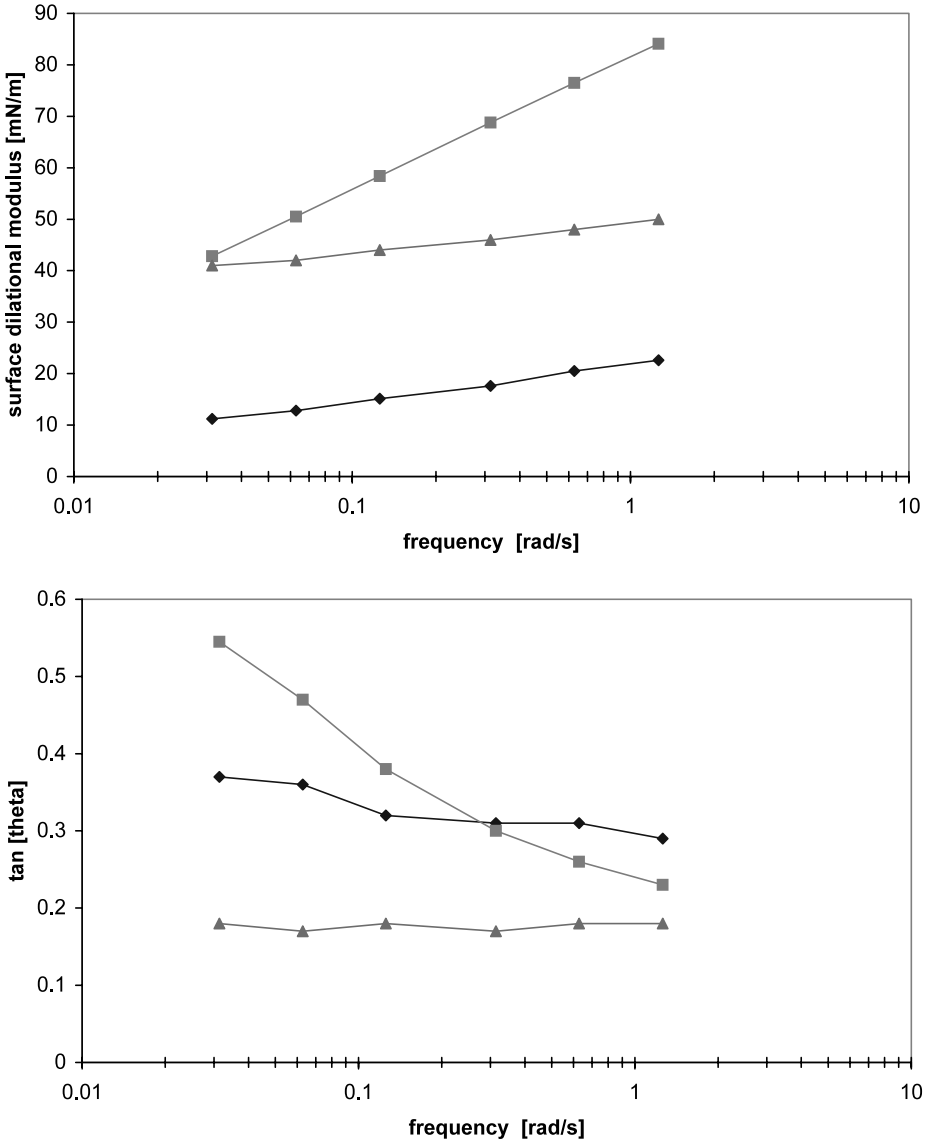

Fig. 3. Surface dilational modulus E and tan θ as a function of angular velocity ω at the air–water interface after equilibration during 2.5 h in the ring trough for β-casein (◆), gliadin (■) and glycinin (▲). Protein concentration was 0.1 g/l, pH 6.7.

therefore also be seen as a measure of the yield/fracture stress of the adsorbed layer [31].

3.4. Langmuir trough with caterpillar belt

While in the overflowing cylinder technique the properties of the protein determine the relative expansion rate of the surface, in Langmuir trough with the caterpillar belt the expansion rate could be set with the speed of the barriers. At a continuously expanding interface, the surface tension quickly reaches a steady state (γ_{dyn}) at which protein adsorption to the expanded interface just compensates the two-dimensional dilution of the adsorbed amount due to interface expansion. The decrease in surface tension compared to water was

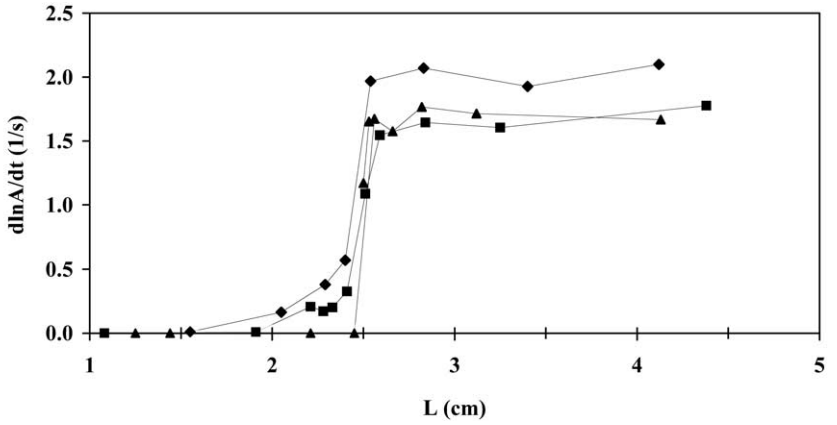

Fig. 4. The relative surface expansion rate d ln A/dt as a function of the length of the falling film L as measured with the overflowing cylinder technique for the air–water interface. β-Casein (◆), gliadin (■) and glycinin (▲). Protein concentration was 0.1 g/l, pH 6.7.

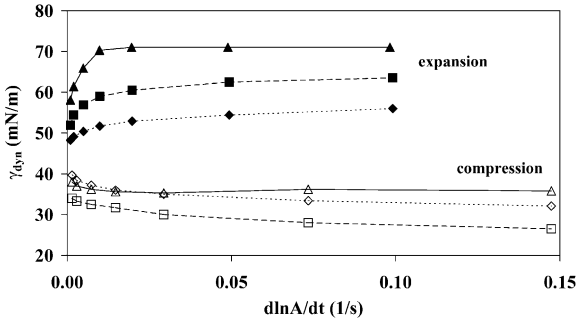

Fig. 5. Dynamic surface tension γ_{dyn} as a function of relative deformation rate d ln A/dt at the air–water interface measured in a Langmuir trough equipped with an endless belt with barriers. Closed symbols showing data in expansion (β-casein (◆), gliadin (■) and glycinin (▲)) and open symbols for compression (β-casein (◇), gliadin (□) and glycinin (△)). Protein concentration was 0.1 g/l, pH 6.7.

dependent on the expansion rate (the rate at which the interface is diluted). Fig. 5 shows the dynamic surface tension γ_{dyn} at an expanding and compressed interface for the three proteins. Differences in γ_{dyn} were clearly observed in expansion and were less pronounced in compression. At high expansion rates glycinin was unable to adsorb in quantities sufficient to lower the surface tension, while at low expansion rates γ_{dyn} was reduced. Gliadin reduced γ_{dyn} only to some extent while β-casein is able to reduce γ_{dyn} very well at an expanding interface. Decreasing the expansion rate increases the ability of all three proteins to adsorb in sufficient quantities at the interface to lower γ_{dyn}, but the extent to which they lower γ_{dyn} stays different. In general, smaller (and more flexible) proteins can lower γ at relatively higher expansion rates than larger (and compact) proteins, because the adsorption rate of the former is higher. Conclusively, the relative rate of adsorption at an expanding interface is similar to that at a static interface for the proteins studied as both methods result in the same order in rate of protein adsorption.

Calculated surface dilational viscosity η_s^d as a function of d ln A/dt obtained with the overflowing cylinder and Langmuir trough with the caterpillar belt showed excellent correspondence when plotted in a double logarithmic graph (Fig. 6). Data obtained with both techniques coincide. The combined data of overflowing cylinder and Langmuir trough can be fitted with a power law, leading to values for the intercept n and the slope m. n was equal for the different proteins about -1.62. However, m differed significantly ($>99\%$ confidence), being -0.82, -0.96 to -0.66 for gliadin, glycinin and β-casein, respectively. η_s^d of all proteins decreases with increasing d ln A/dt, meaning that the interface becomes thin fluid-like with increasing deformation rate, comparable to shear rate-thinning behaviour in bulk rheology. For β-casein, η_s^d deviates from the power line at low d ln A/dt to a plateau value as is seen in the

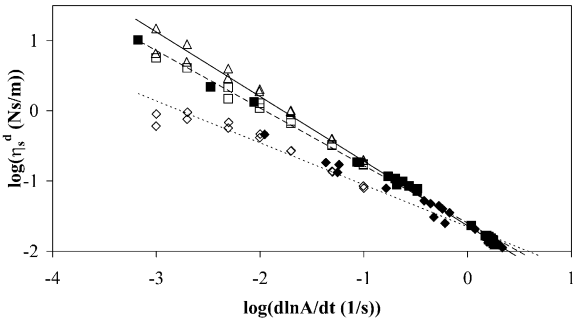

Fig. 6. Surface dilational viscosity η_s^d as a function of d ln A/dt for air–water interfaces. Open symbols (β-casein (◇), gliadin (□) and glycinin (△)) measured with a Langmuir trough equipped with an endless belt with barriers and closed symbols with the overflowing cylinder. Protein concentration was 0.1 g/l, pH 6.7. The lines drawn are the power law fits. Dotted line, β-casein; broken line, gliadin and solid line, glycinin.

first Newtonian plateau in bulk rheology of polymer solutions and melts.

3.5. Bursting membrane

The interfacial pressure π of an oil–water interface increased rapidly after bursting of the membrane in case of β-casein and gliadin, but not for glycinin (Fig. 7). π reached a plateau value for β-casein within the time scale of the experiment, but not for gliadin and glycinin. The increase in surface pressure as function of time of the proteins clearly increases in the order glycinin < gliadin < β-casein, in agreement with the data obtained for adsorption at the air–water interface and the observed increase in E as a function of time. This indicates that the relative rate of adsorption at an oil–water interface protein is affected by the same protein characteristics as at the air–water interface. As a consequence, it can be concluded that also for the oil–water interface the adsorption rate is mainly determined by molecular size and structure.

3.6. Foam tests

Producing a good foam depends on the amount of protein present and the experimental technique with which the foam is produced. Comparing, e.g., whipping, shaking and gas sparging, the amount of protein required for foam production is less for gas sparging and shaking than for whipping [32]. In this study, shaking was used to determine foam formation by the three proteins. At protein concentrations of 0.1 g/l, formed foam volumes were so small that results were not reliable and reproducible. Foam volumes obtained at a concentration of 1.4 g/l were well reproducible. Results are

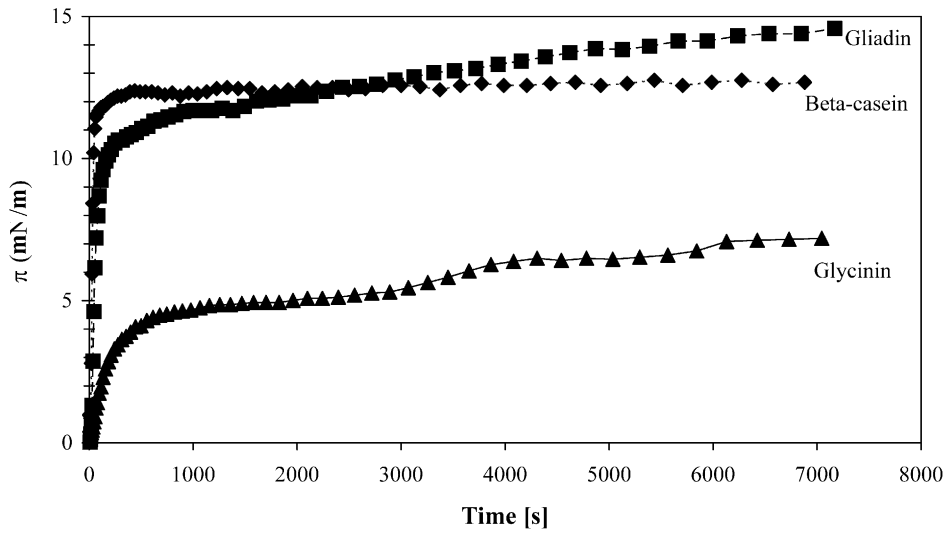

Fig. 7. Interfacial pressure Π of the oil–water interface as a function of time t after bursting of the membrane in bursting membrane technique; β-casein (◆), gliadin (■) and glycinin (▲). Protein concentration was 0.1 g/l, pH 6.7.

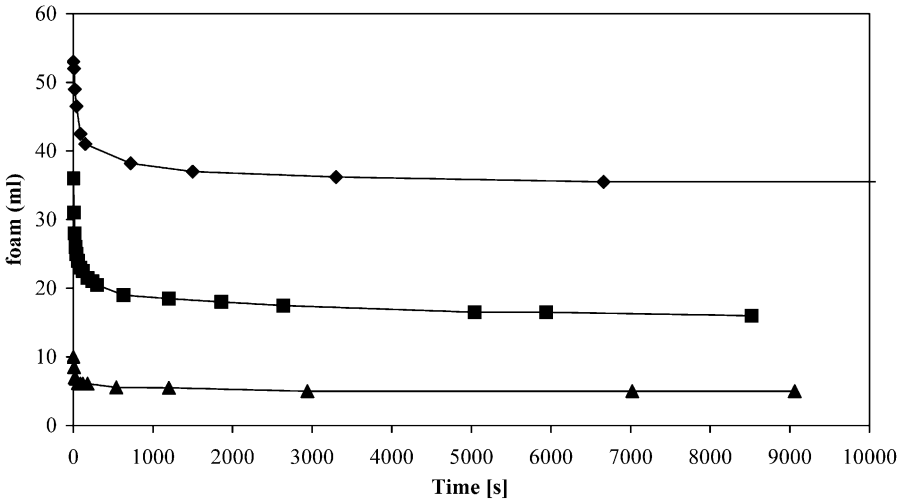

Fig. 8. Foam volume as a function of time for β-casein (♦), gliadin (■) and glycinin (▲). Protein concentration was 1.4 g/l, pH 6.7.

plotted as a function of time in Fig. 8. The initial volume clearly increases in the order glycinin < gliadin < β-casein. β-Casein and gliadin formed very fine foams whereas glycinin formed a coarse foam.

The difference in ability to produce foam between the proteins studied can be explained by the difference in adsorption rate observed at either static (Fig. 1) or expanding interfaces (Fig. 5) and the rigidity of the protein. Because of its high molecular weight and rigid structure, glycinin (pH 6.7) does not adsorb and unfold sufficiently fast enough at the interface and to produce much foam. This is in line with what was found by Martin et al. [16]. They also showed that, by altering the pH of the solution to pH 3, foamability of glycinin could be enhanced dramatically. This enhancement could be correlated to a different protein structure at pH 3.0.

4. Conclusion

Interfacial rheological properties and their suitability for foam production and stabilisation were studied for two vegetable proteins (gliadin and soy glycinin) and compared to β-casein. Although gliadin exhibits the highest dilational modulus, followed by glycinin and β-casein, glycinin formed the strongest film against fracture in the overflowing cylinder.

Gliadin had the lowest equilibrium interfacial tensions and β-casein the lowest dynamic surface tension during expansion. Hardly any foam could be formed at a concentration of 0.1 g/l by shaking. At a concentration of 1.4 g/l, most foam was formed by β-casein, followed by gliadin and glycinin. It seems that in the first place the rate of adsorption is important for foam formation. For the vegetable proteins, adsorption was slow. This resulted in lower foamability, especially for glycinin. The network forming properties of vegetable proteins were stronger than for β-casein, although this was not reflected in the foam stability.

References

[1] S. Utsumi, Y. Matsumura, T. Mori, in: S. Damodaran, A. Paraf (Eds.), Food Proteins and their Applications, Marcel Dekker, New York, 1997 (Chapter 3).
[2] D. Marion, L. Dubreil, P.J. Wilde, D.C. Clark, in: R.J. Hamer, R.C. Hoseney (Eds.), Interactions: The Keys to Cereal Quality, AACC, St. Paul, Minnesota, 1998 (Chapter 6).
[3] D.E. Graham, M.C. Philips, J. Colloid. Interf. Sci. 76 (1980) 240.
[4] J. Benjamins, E.H. Lucassen-Reynders, in: D. Möbius, R. Miller (Eds.), Proteins at Interfaces, Elsevier, Amsterdam, 1998 (Chapter 9).

[5] E. Dickinson, Colloid. Surf. B 15 (1999) 161.
[6] M. Hammershoj, A. Prins, K.B. Qvist, J. Agric. Food Sci. 79 (6) (1999) 859–868.
[7] A.R. Mackie, A.P. Gunning, P.J. Wilde, V.J. Morris, J. Colloid. Interf. Sci. 210 (1999) 157–166.
[8] M. Kooijman, M. Hessing, R. Orsel, R.J. Hamer, A.C.A.P.A. Bekkers, J. Cereal Sci. 26 (1997) 145.
[9] M. Kooijman, R. Orsel, R.J. Hamer, A.C.A.P.A. Bekkers, J. Cereal Sci. 28 (1998) 43.
[10] J.J. Kokelaar, J.A. Garritsen, A. Prins, Colloid. Surf. A 95 (1995) 69.
[11] T.A. Paternotte, R. Orsel, R.J. Hamer, J. Cereal Sci. 19 (1994) 123.
[12] J.-P. Krause, R. Mothes, K.D. Schwenke, J. Agric. Food Chem. 44 (1996) 429.
[13] S.H. Kim, J.E. Kinsella, J. Food Sci. 52 (1987) 128–131.
[14] J. Guégen, S. Bollecker, K.D. Schwenke, B. Raab, J. Agric. Food Chem. 38 (1990) 61.
[15] M.A. Bos, A. Martin, J. Bikker, T. van Vliet, in: E. Dickinson, R. Miller (Eds.), Food Colloids, Fundamentals of Formulation, Royal Society of Chemistry, Cambridge, 2000, p. 223.
[16] A.H. Martin, M.A. Bos, T. van Vliet, Food Hydrocolloids 16 (2002) 63.
[17] V.H. Tanh, K. Shibasaki, J. Agric. Food Chem. 24 (1976) 1117.
[18] C.M.M. Lakemond, H.H.J. De Jongh, M. Hessing, H. Gruppen, A.G.J. Voragen, J. Agric. Food Chem. 48 (2000) 1991–1995.
[19] J.J. Kokelaar, A. Prins, M. de Gee, J. Colloid. Interf. Sci. 146 (1991) 507.
[20] D.J.M. Bergink-Martens, H.J. Bos, A. Prins, B.C. Schulte, J. Colloid. Interf. Sci. 138 (1990) 1.
[21] F.J.G. Boerboom, Ph.D. Thesis, Wageningen University, The Netherlands, 2000.
[22] A. Prins, F.J.G. Boerboom, H.K.A.I. van Kalsbeek, Colloid. Surf. A 143 (1998) 395.
[23] J. Lyklema, Fundamentals of interface and colloid science, in: Y.P.S. Bajaj (Ed.), Liquid–Fluid Interfaces, vol. III, Academic Press, London, 2000 (Chapter 3).
[24] M. Stang, H. Karbstein, H. Schubert, Chem. Eng. Process. 33 (1994) 307–311.
[25] A. Martin, K. Grolle, M.A. Bos, M.A. Cohen Stuart, T. van Vliet, J. Colloid. Interf. Sci. 154 (2002) 175–183.
[26] F. Yamauchi, T. Yamagishi, S. Iwabuchi, Food Rev. Int. 7 (1991) 283–322.
[27] J. Benjamins, A. Cagna, E.H. Lucassen-Reynders, Colloid. Surf. A 114 (1996) 245.
[28] C.-S. Gau, H. Yu, G. Zografi, J. Colloid. Interf. Sci. 162 (1994) 214.
[29] D.E. Graham, M.C. Philips, J. Colloid. Interf. Sci. 70 (1979) 427.
[30] A. Williams, A. Prins, Colloid. Surf. A 114 (1996) 267.
[31] M.A. Bos, K. Grolle, W. Kloek, T. van Vliet, Langmuir 19 (2003) 2181–2187.
[32] J.B. German, L. Phillips, in: N.S. Hettiarachchy, G.R. Ziegler (Eds.), Protein Functionality in Food Systems, IFT Basic Symposium Series, Chicago, IL, 1991, p. 181.